J Mater Sci (2011) 46:4880–4895
DOI 10.1007/s10853-011-5400-4

Design and microstructural analysis of magnesium alloys for dynamical applications

V. G. Tkachenko · K. H. Kim · B. G. Moon · A. S. Vovchok

Received: 1 November 2010 / Accepted: 16 February 2011 / Published online: 25 February 2011

Abstract A microanalytical characterization of cast magnesium alloys of eutectic origin based on the Mg–Al–Ca ternary matrix system has been carried out in order to investigate the influence of alloying elements on their microstructure as well as microchemistry-processing-microstructural relations using structure-sensitive techniques of electron microscopy, mechanical spectroscopy (internal friction), X-ray diffractometry, and advanced microanalytical methods including electron probe compositional analysis. Following the data obtained here there is direct correlation of microstructure with creep properties of the new experimental magnesium alloys. The creep and heat-induced properties of the multicomponent magnesium alloys containing low range of inexpensive additions of titanium (0.07–0.2%) or strontium (of about 1.8%) are defined by resulting structure dynamically formed during creep strain (up to 200 h). It is noteworthy that Ti as novel alloying element competes for creep resistance and cost with Sr and attracts as-cast desirable properties minimizing solute effects at ambient temperatures because of the pinning of slowly moving dislocations with the binding energy no more then 0.3 eV as well as because of stress-induced strengthening. The Ti and Sr solute atmosphere dragging is believed to be the rate-controlling mechanism responsible for radical improvement of creep resistance and long-term strength in the newly developed magnesium alloys at elevated temperatures. The new experimental alloys are superior to commercial alloys AZ91D, AE42, and AS21 following their creep resistance, long-term strength, heat resistance, and castability because of their novel microstructure having desirable engineering properties for structural applications (creep strain ε_c less than 0.3–0.4% at 423 K and 70 MPa for 200 h; $\dot{\varepsilon}_c \sim 10^{-9}$ s^{-1}). The newly developed magnesium alloys with improved castability could be used in die-casting technology and automobile (powertrain) industry for manufacturing of components and parts which are difficult to cast with more desirable microstructure.

V. G. Tkachenko (✉) · A. S. Vovchok
International Center for Electronic Materials Science and Applied Problems of Aerospace Technology,
3 Krzhizhanovsky str, 03142 Kiev-142, Ukraine
e-mail: icems@ipms.kiev.ua

K. H. Kim · B. G. Moon
KIMM, 531, Changwondaero, Changwon,
Gyeongnam 641-831, Korea

Introduction

The material selection for automobile design and mass production is one of the most critical problems connected with competition for abundant inexpensive raw materials supply. Research on die-casting technology has reached a status where in design studies the basic requirements for the highly loaded materials have been identified. The requirements of the affordable cost and good die castability of new experimental magnesium alloys reduce possible options to alloying systems which are containing Al and Zn as major elements and Mn, Si, Ca, Sr, RE as relatively small additions [1]. Much progress has been made [1, 2] but, nevertheless, any attempts to design magnesium alloy systems consisting of inexpensive alloying elements (AE) face some problems that concern definition of secondary processing issues such as limited plasticity at r.t., decreased corrosion resistance, soldering with a mold in a die-casting technology, welding and joining (enhanced diffusion bonding) of parts/products/panels constructed of them.

The new magnesium alloys in Mg–Al–Ca–X system which have been developed in recent years for use as

functional and structural materials in engineering applications could perform well in engine and transmission cases [1–5]. They have been attracting attention because of their desirable engineering properties such as creep resistance and long-term strength at elevated temperatures during long-term usage as well as because of their greater potential for weight savings, for example, in automobile industry. No insurmountable problems have arisen so far. Nevertheless, more work with the Mg–Al–Ca system is needed to optimize composition of the magnesium alloys containing Ca for die-casting. Mg–Al–Ca system must be further investigated for optimum castability. Furthermore, in the range of investigated compositions and usual casting the addition of Ca leads to an excessive hot-cracking and die-soldering especially in Mg–Al–Ca alloys containing the small addition of Al and above 1 wt% Ca [3]. Subsequent addition of 8 wt% Zn causes improvement of the die castability but the creep properties were founded to vary over a wide range [6]. Hence, additional fundamental and applicable research is required in all areas of magnesium production in order to substantially increase the use and applications of magnesium alloys basing oneself on the synergetic effect of magnesium processing and alloy development.

The work is a continuation of a cooperative effort of the ICEMS, Ukraine and the KIMS, Republic of Korea for the purpose of evaluating and comparing the creep properties of newly developed magnesium alloys and of verificating their processing-composition-microstructure-property relationship. The main purpose of this article is to develop new experimental die casting magnesium alloys Mg–Al–Ca–X system with higher castability, more excellent creep resistance and higher long-term creep strength at larger stress and higher temperature (70 MPa and 423 K) by carrying out their full-scale research, observation and testing standards driven to low cost applications and mass productions. It is likewise the intention of this study to subject the measurements to a complete analysis regarding phase composition and dislocation density changes during creep testing (in stress field). For better understanding of solidification structures and for attaining the stated final result both research groups of Ukraine and Korea are going in future to identify of rate-controlling creep mechanisms responsible for power law and thermally activated (Arrhenius) behavior of the alloys to be investigated in a wide temperature range of 293–523 K for automotive power train, oil pump, and other advanced commercial applications.

Experimental procedure

Out previous investigations of phase equilibria in the ternary Mg–Al–Ca system studied by the methods of differential thermal (DTA), X-ray diffraction (XRD), electron-probe and microscopic analysis have resulted in constructing the isothermal section at 423 K and polythermal sections at 4.5, 8.5, and 16 mass% Al [7]. Additions of Al and Ca were introduced to decrease the liquidus temperature of the magnesium alloys from 923 to 711 K. It was shown that the three-phase region $< Mg > + < Al_2Ca > + < Mg_{17}Al_{12} >$ exists at 423 K with corresponding two-phase fields, temperature dependence of the homogeneity range of the α–Mg solid solution as well as temperatures of the phase transformations which occur in the investigated system.

As reported in [8], creep rate decreases, and long-term strength increases with increasing rate of crystallization (RC) of the eutectics because of the dispersion hardening mechanism. Therefore, magnesium alloys were synthesized and produced under non-equilibrium conditions of crystallization at cooling rate of about 333 K per sec. Used as the additional alloys to cast different magnesium alloys based on Mg–Al–Ca–X system of eutectic origin were the Mg–30%Ca, Al–10%Ti, and Al–10%Sr master materials. The new experimental alloys were prepared by melting stoichiometric amounts of the constituent elements in an induction melting furnace (additional alloys) and then in an electrical resistance heating furnace under flux (ingot casting) using argon as well as CO_2 with 0.5% SF_6 to protect the melt from oxidation. They were melted in graphite crucibles; the molten alloys were held at 1013 K and then poured into the permanent copper mould ø 6 × 60–70 (mm).

Measurements of castability for magnesium alloys were carried out using an original installation (on the basis of induction vacuum furnace), which is encapsulated, pumped and filled with inert gas (99.998%Ar). During melting of an alloy of 50 g in mass excess the pressure of argon makes up about 0.2–0.4 atm gage. After melting the liquid alloy is maintained during 10 min under the excess pressure, which is controlled with accuracy of 0.01 atm by precision manometer. Length of a sample is measured (in mm) after its cooling up to r.t. When comparing data obtained the vacuum suction casting temperatures should be in excess of 323 K (over liquidus curves) for all the magnesium alloys under investigation [2, 9]. The results obtained are much the same as compared with the result that is produced by using complex U-shaped sample in well-known Nekhendzi–Kuptsov method under the stabilized conditions of the experiment: of about 63 mm for AZ91D industrial alloy and 90 mm for Mg–12.5Al–1.3Ca–0.28Mn–0.2 Ti alloy at pouring temperature of 873 K.

The dislocation structures in as-cast magnesium alloys produced were characterized by TEM observations. Their examination was carried out using a well-know technique [10, 11]. Scanning electron microscopy was used to perform X-ray electron probe analysis of their surface [12].

Torsional experiments were performed on samples having a gauge length of 70 mm length and of 1 mm in diameter.

The variation of internal friction, $Q^{-1}(T)$ in magnesium alloys as a function of temperature was studied in the range of 293–800 K by the free-decay method, as developed by Ke [13]. Discrete temperature spectra of internal friction for magnesium and its alloys were recorded by using the relaxometer such as inverted-torsion pendulum operating in the low frequency range (at 1 Hz) and constant strain amplitude of 1×10^{-5} in the mode of free-damping torsional vibrations.

As is known, $Q^{-1}(T)$ background displaces exponent, which is dependent on properties of mobile dislocations in the bulk solid solution so that high temperature internal friction is independent of strain amplitude and appears to follow a low of the type [14]:

$$Q^{-1}(T) = A\exp(-U/kT) \quad (1)$$

The apparent activation energy (a.e.) of the internal friction is obtained by plotting $\ell n\ Q^{-1}$ vs. 1/T which gives a straight line, if Eq. 1 is obeyed because of some thermally activated dislocation relaxation or diffusion–controlled dislocation relaxation that are responsible for the energy dissipation.

Amplitude dependent damping attributed to dislocations [15] was measured with increasing strain amplitude γ up to 5×10^{-4}. The binding energy E_b for dislocation-solute interaction was calculated from experimental data via the conventional form of the linear equation which states that $\ell n\ tg\alpha$ vs. 1/T plot should produce straight line with the slope of E_b/k.

$$Q^{-1} = Q_0^{-1} + tg\alpha \cdot \gamma \quad (2)$$

Dislocation damping measurements have been performed on the as-cast magnesium alloys in order to determine the values of the binding energy between solute atoms and pre-existing dislocations at temperatures ranging from 293 to 733 K.

The standard X-ray phase analysis of the new experimental alloys was performed using diffractometer DRON-UM1 with monochromatic CuK_α–radiation and monocrystal of graphite as monochromator located in the place of secondary beam. Stepwise X-ray registration with angle step of 0.05° was employed for determination of lattice parameters. Approximation of diffraction profiles was carried out through psevdo–Foght function by means of LS-variation of their K—component angle position, integral intensity, half-width, and asymmetry. CIB programs package was employed for the more precise lattice parameters calculation. The correction of X-ray penetration into a sample depth has been taken into account. A peak-breadth analysis has allowed to estimate the volume-weighted crystalline size and a microstrain averaged all over the coherence length to be perpendicular to the diffracting planes [16].

The precise X-ray diffraction studies were carried out using a continuous drive diffractometer to characterize the dislocation densities of a magnesium alloy before and after small creep strain (up to 0.5%) for better understanding the rate-controlling creep mechanism. In a combination with graphite monochromater as a filter providing a divergence and width of beam to be up to standard of 50 angular second and no more than 0.15 mm, respectively, XRD measurement parameters (angle interval, step length, etc.) as well as X-ray diffraction peak-boardening analysis were employed to single out lattice distortions. This is well-known advanced technique and its main features have been reviewed in the textbooks [17, 18]. All data have been collected by using CuK_α radiation and by operating the X-ray diffractometer equipment in a step scan mode with 0.01° in 2θ per step. Under this provision, the peak width could be measured with the accuracy of ± 0.01° in 2θ.

Short-range tensile tests were performed at a constant cross-head speed giving an initial strain rate of 10^{-3} s^{-1} at temperature of interest. Creep tests were carried out in tension using a constant lever arm tester and a temperature averaging extensometer, which employs a super linear variable capacitor to measure the strain. Cylindrical tensile specimens 3 mm in diameter and 25.4 mm gage length were machined from as-cast material. The apparent a.e. for creep Q_c was determined experimentally from an Arrhenius relationship where the logarithm of the long-term creep strain rate $\dot{\varepsilon}_c$is plotted against the reciprocal of temperature [19]:

$$\dot{\varepsilon}_c = A\sigma^n \exp(-Q_c/RT) \quad (3)$$

The values of Q_c and the stress exponent n are necessary to identify thermally activated (rate-controlling) mechanism in a particular temperature and stress rate ranges.

Experimental results

General microstructural characterization of new experimental as-cast alloys

X-ray measurements of lattice parameters presented in Table 1 indicate the presence of solid solutions in terms of α–Mg and β–$Mg_{17}Al_{12}$ structural components, as has been claimed by Massalski [20]. The data obtained are in a good agreement with the refined lattice parameters for HCP Mg and its alloys in systems Mg–Al and Mg–Al–Zn [21]. It is obvious that their lattice distortions are compositional-dependent. It is very difficult to elucidate the physical nature of the solid solutions because of complexity of determining factors that contribute to mutual solubility of

Table 1 Lattice parameters of α-Mg and β-$Mg_{17}Al_{12}$ phases in magnesium alloys of eutectic origin

Metal alloy system	α-Mg solid solution		β-$Mg_{17}Al_{12}$		Standards for verification
	a, nm	c, nm	a, nm	volume fraction, in vol.%	
Mg–12.5Al	a = 0.31650	c = 0.51454	a = 1.05463	25.5	HCP Mg: sp.gr.$P6_{3/mm}$ a = 0.32093 nm
Mg–12.5Al–1.3Ca	a = 0.31730	c = 0.51574	a = 1.05883	11.2	c = 0.52112 nm c/a = 1.62375
Mg–12.5Al–1.4Ca–0.3Mn–0.1Ti	a = 0.31724	c = 0.51546	a = 1.05883	14.2	c/a = 1.633 (ideal value) [20, 21]
Mg–12.5Al–11.7Sr–0.3Mn–0.1Ti	a = 0.31735	c = 0.51540	a = 1.05633	11	$Mg_{17}Al_{12}$ (sp.gr. I–43 m) with BCC lattice of α–Mn type: a
Mg–12.5Al–1.3Ca–0.3Y–0.1Gd	a = 0.31715	c = 0.51528	a = 1.05892	18.75	=1.05438 nm [21, 22]

solute and solvent atoms without attracting of the concepts concerning electron structure and relative valency rule. Nevertheless, there is a tendency to contraction of the distorted lattices for the both structural components (Table 1) thereby testifying to some interaction between solute and solvent atoms. In any case relative valency and chemical affinity seem to be important factors upon alloying magnesium with additions under investigation, as previously indicated [20]. Standard X-ray analysis has revealed only two-phase structure of eutectic origin consisting of decaying α–Mg solid solution enriched by soluble AE as well as much more refractory β–$Mg_{17}Al_{12}$ strengthened by the same AE. Volume fraction of β–$Mg_{17}Al_{12}$ in new experimental magnesium alloys based on Mg–12.5Al–1.3Ca matrix ranges 11.2–18.8 vol. per cent, if amount of the additional AE such as Ti, Gd, Y does not exceed 0.1–0.3 wt% (Table 1).

The practical interest to microstructures of eutectic origin arises from the chemical equilibrium of two phases, e.g., α–Mg and β–$Mg_{17}Al_{12}$, which are unaffected by chemical decay [23, 24]. Moreover, they have phase interfacial bonding capable of effectively transferring a load from one phase to the other phase called natural eutectic strengthening. The microstructure of eutectic origin compares favorably with their thermal stability due to formation during a solidification of low energy phase-to-phase states, which makes them good for creep resistance. Magnesium alloys of Mg–Al–Zn and Mg–Al–Mn systems are characterized by divorced eutectics. Increase of the strengthened β–$Mg_{17}Al_{12}$ volume fraction in magnesium alloys of Mg–Al–Ca system (up to 18.8 vol%) seems to cause an additional (natural) eutectic strengthening. It is noteworthy that the experimental magnesium alloys especially those containing small additions of Y and Gd are phase-stable at least up to 430 K (volume fraction of 18.8% at 293 K against 18% at 430 K for Mg–12.5Al–1.3Ca–0.3Y–0.1Gd alloy). It is not at all essential to examine in detail the observed dislocation structure which is present in as-cast magnesium alloys following TEM observations (Fig. 1a, b). The main thing is to examine the dynamic dislocation—alloying element interaction that is responsible for creep property. It therefore seems appropriate to continue work along these lines basing oneself on advanced structure-sensitive techniques. The dislocation microstructure will be sound by highly dynamic structure-sensitive

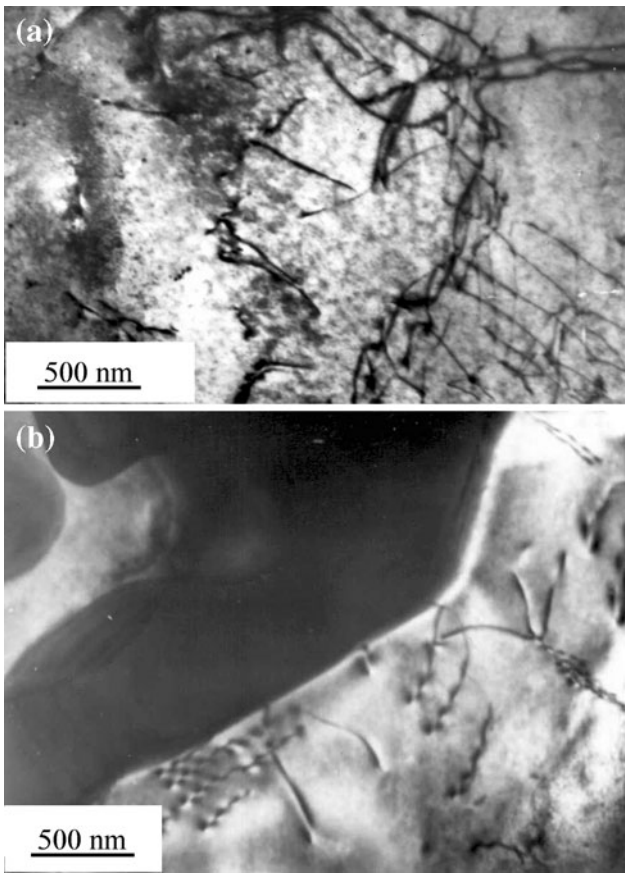

Fig. 1 Typical dislocation structures which are formed in the bulk α–Mg grain (**a**) and near the interface of the $Mg_{17}Al_{12}$ phase (**b**) of as-cast alloy of Mg–Al–Ca system produced by rapid solidification technique

methods of internal friction with mechanical spectroscopy and amplitude dependent damping involved.

Internal friction measurements

The internal friction of magnesium alloys under investigation was measured as a function of their chemical composition based on Mg–Al–Ca-basic matrix. The results of the measurements are presented in Figs. 2, 3, 4.

Structural studies by mechanical spectroscopy (Fig. 2) yield a discrete temperature spectrum of internal friction with a broad inelastic maximum of relaxation origin which may be decomposed into two main components produced by grain boundary (GB) relaxation [25, 26]. The first temperature peak at 460 K is associated with GB dislocation-induced relaxation while second one at 480 K is attributed to GB solute segregation-induced relaxation. The experimental profile and experimental points (around 460 K) of the abroad maximum indicate that the same GB peak with a.e. of about 1.3 eV has appeared as those already found at 458 K and 483 K for doubly sublimated HCP Mg of high purity and for conventional HCP Mg, respectively [27, 28].

The width of the GB maximum $Q^{-1}(T)$ in the as-cast magnesium essentially exceeds its theoretical value by reason of the existence of inevitable impurities in HCP Mg. The authors have noticed that their segregation at the GBs seems to cause additional GB segregation-induced relaxation at higher temperatures [29, 30]. Therefore, the higher temperature 483 K-peak within the maximum of Q^{-1} (T) seems to be a consequence of the influence of inevitable impurities such as solute hydrogen and oxygen [25, 26]. The effect of the GB segregation-induced inelastic relaxation to some extent masks the original GB dislocation-induced relaxation peak itself. Moreover, the existence of relaxation time spectrum and grain-size distribution, which are typical for any as-cast metal alloy system also changes intensity of the both original GB dislocation-induced relaxation itself and GB solute segregation-induced relaxation itself.

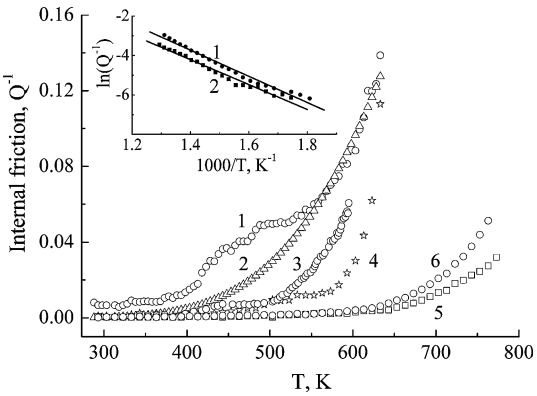

Fig. 2 Discrete temperature damping spectra of as-cast magnesium (99.96%) and its alloys investigated at low frequency vibrations of about 1 Hz (1 cps):*1* magnesium, *2* Mg–2Ca, *3* Mg–12.5Al, *4* Mg–12.5Al–1.3Ca, *5* Mg–4.9Al–0.28Mn–1.8Sr, *6* Mg–12.5Al–1.4Ca–0.28Mn–0.1Ti. *Inset* processing of the background-produced experimental data to evaluate the apparent a.e. U_a of the rate-controlling mechanism at higher temperatures: *1* Mg–12.5Al–1.4Ca–0.28Mn–0.1Ti testified by $U_a = 0.57$ eV, *2* Mg–4.9Al–0.28Mn–1.8Sr testified by $U_a = 0.54$ eV

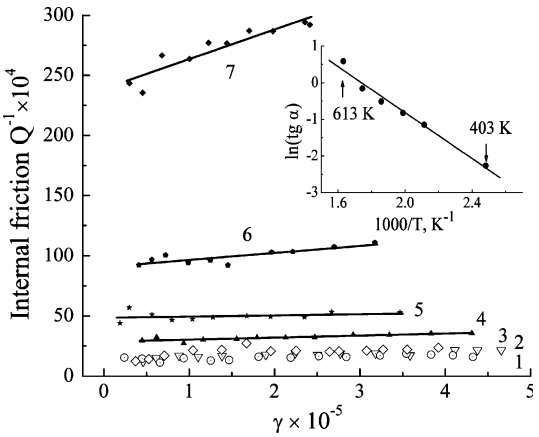

Fig. 3 Variation of internal friction with strain amplitude at different temperatures for Mg–12.5Al–1.4Ca–0.28Mn–0.1Ti alloy: *1* 293, *2* 363, *3* 403, *4* 448, *5* 503, *6* 563, *7* 633 K. *Inset* linear relationship between slope of ℓn tg α and reciprocal temperature for determining the dislocation-solute binding energy testified by $E_b = 0.27$ eV

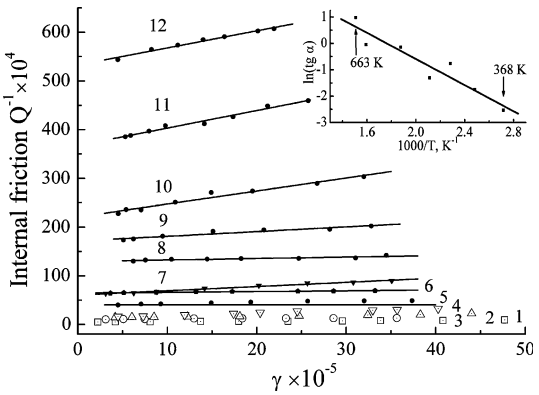

Fig. 4 Variation of internal friction with strain amplitude at different temperatures for Mg-4.9Al-0.28Mn-1.8Sr alloy: *1* 293, *2* 368, *3* 403, *4* 438, *5* 473, *6* 503, *7* 533, *8* 583, *9* 628, *10* 663, *11* 703, *12* 733 K. *Inset* linear relationship between slope of ℓn tg α and reciprocal temperature for determining the dislocation-solute binding energy testified by $E_b = 0.21$ eV

Detailed structure consisting of GBs dislocations is vitally important in understanding GB sliding and creep properties of the magnesium alloys studied. Some localized strain is apparent near the interface between α–Mg and β–$Mg_{17}Al_{12}$ phases (Fig. 1b). The evidence for GB sliding derives principally from damping measurements (Fig. 2) according to a model of viscous sliding in analogy to the

GB sliding suggested for polycrystalline FCC Al [31]. Intensity of GB dislocation-induced relaxation is determined by density of GB dislocations [29, 30]. Introduction of calcium is succeeded by effective suppression of the both types of GB relaxation in magnesium alloys of Mg–Ca and Mg–Al–Ca systems (Fig. 2 curve 1, 2, 3 and Table 2). The process is completed by blocking GB dislocations and GB strengthening because of thermal and stress-induced segregation of calcium to the GBs.

Following the amplitude-dependent internal friction (ADIF) data (Figs. 3 and 4) for magnesium alloys containing 0.1% Ti and 1.8% Sr the procedure reveals temperature of the Cottrell's atmosphere condensation on dislocations ($T_0 \sim 453$–473 K), which divides regions of the thermally activated pinning (at lower temperatures) and the thermally activated unpinning of dislocations from the solute atmosphere (at higher temperatures). It is evident that pre-existing dislocations typical for as-cast structure have already been pinned upon rapid crystallization seeing that $\mathrm{tg}\alpha \sim$ const at lower temperatures $T < T_0$ (Figs. 3, curves 1–4 and 4, curves 1–6). In the lower temperature range where dislocation relaxation is dominant rate-controlling mechanism, and time-dependent microdeformation is controlled by dislocation creep, microstructural changes in as-cast microstructure are succeeded by thermal stabilization of α–Mg solid solution upon additional alloying with Ti and Sr. It follows that Ti and other similar atoms (Table 3) interact preferentially with pre-existing dislocations with binding energy E_b which is large enough to maintain the dislocation atmospheres at temperatures lower than certain of the dense atmosphere condensation, T_0 to be different for various magnesium alloys. Microsegregation of the AE such as Ti and Sr occurs during rapid solidification and continues under coding and even subsequent heat treatment by analogy with other non-equilibrium metal alloy system with well-defined short-range order.

Thermally activated unpinning of the dislocation is certain to occur with increasing temperature $T > T_0$ (Figs. 3, curves 5–7 and 4, curves 7–12). The statement is supported by the increase in $\mathrm{tg}\alpha$ with increasing temperature. At higher temperatures $T > T_0$ the atmospheres begin to decompose by the unpinning dislocation mechanism. In any case for as-cast microstructure with decaying α–Mg solid solution, the apparent a.e. calculated from high-temperature Q^{-1} background data (Fig. 2, insert and Table 2) are in a good agreement with the a.e. obtained for β–$Mg_{17}Al_{12}$ precipitation reaction at elevated temperatures [32, 33].

It is significant that additions of Ti and Sr with negligible and limited solubility in HCP Mg, respectively, shift their transition points to the high-temperature background of internal friction (Fig. 2, curves 5 and 6) demonstrating essential increase in heat-resistance (approximately by 393–433 K). Thus, their segregation on dislocations extend temperature ranges of existence of thermally stable microstructure.

Microchemistry—microstructure-property relationship

Using the precise X-ray diffractometry the authors succeeded in obtaining the data of microstructure changes and progressive phase transformations arising during small creep strain at 423 K under tensile stress of 70 MPa for magnesium alloys in Mg–Al–Ca–Y system. The idea of stress-induced strengthening is supported by XRD analysis of a microstructure after creep strain (Figs. 5, 6, 7). The observed θ–2θ XRD patterns of the Mg–12.5Al–1.4Ca alloy with addition of 0.3Y taken in the angle range $18° < 2\theta < 80°$from specimen in as-cast (unstrained) condition (1), after creep strain of 0.3% (2), in the region excluding necking as much as 0.5% (3), and in the neck after creep strain of 0.5% (4) are illustrated in Fig. 5. As seen from this figure (curves 1, 2, and 3), in case the creep strain does not exceed 0.4% no change in its phase constitution and lattice distortion (dislocation) density appears

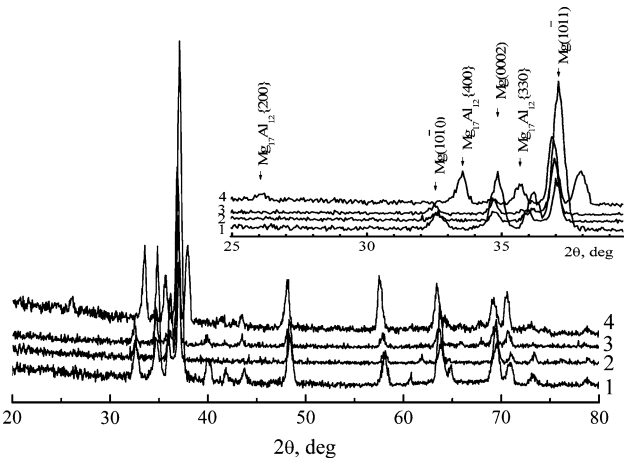

Fig. 5 XRD patterns in the relative intensity, % -2θ, degree coordinates for the Mg–12.5Al–1.4Ca –0.3Y alloy: (*1*) as-cast state (deformation-free head) and *2*, *3*, *4* after total creep strain 0.3% (*2* generatrix) 0.5% (*3* generatrix), and 0.5% (*4* neck) under tensile stress 70 MPa at 423 K

Table 2 Apparent background energy U_a as a function of alloy composition

Alloy composition	Mg (99.96%)	Mg–1.5Ca	Mg–12.5Al–1.3Ca	Mg–12.5Al–1.4Ca–0.28Mn–0.1Ti	Mg–4.9Al–0.28Mn–1.8Sr
U_a, eV	0.30	0.47	0.66	0.57	0.54

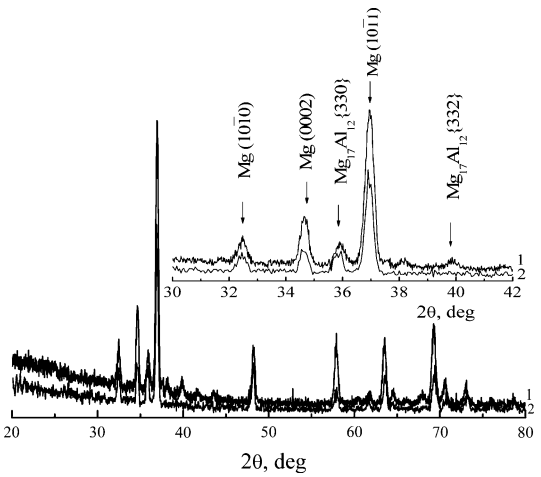

Fig. 6 XRD patterns of the Mg–12.5Al–1.4Ca–0.28Mn–0.1Ti alloy: *1* as-cast state (deformation-free head), *2* after total creep strain 0.37% under tensile stress 70 MPa at 423 K

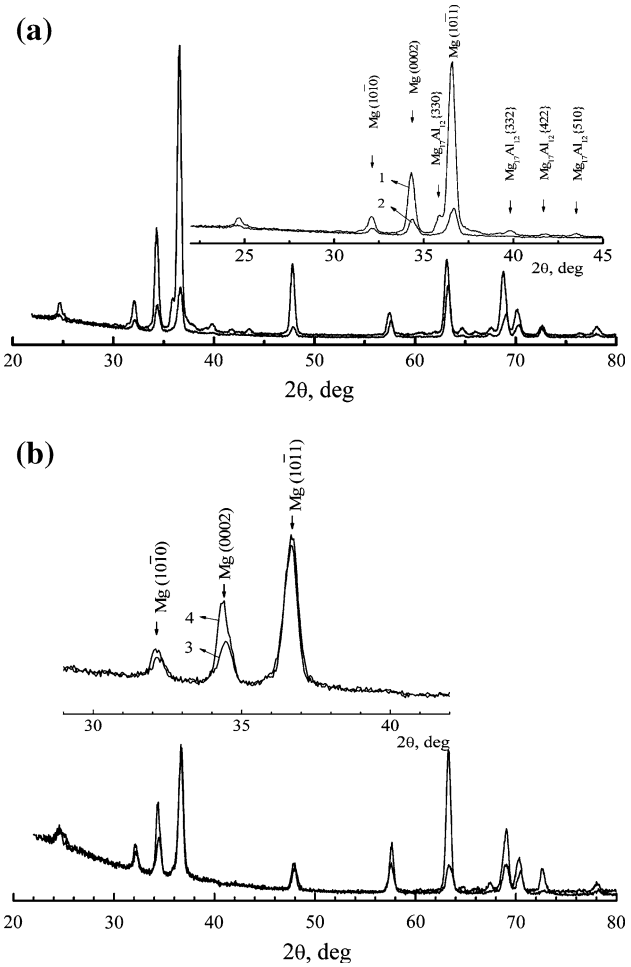

Fig. 7 **a**, **b** XRD patterns of the Mg–12.5Al–1.4Ca–0.28Mn–0.1Ti alloy: *1* as cast state (deformation-free head), *2*, *3* after total creep strain accumulated during long-term test for 200 h under tensile stress 70 MPa at 423 K (*3* generatrix and *4* cross-section)

to occur. As a matter of fact, the authors observe actual coincidence of the diffraction angles for most reflections, slight redistribution of their observed intensity and insignificant change of their half- width as a measure of its physical state upon deformation. Undoubtedly, the stable behavior of the Mg–Al–Ca–Y alloy before its necking is supported by strong resemblance of X-ray lines for specimens in unstrained and creep strained conditions. By contrast, in case the necking occurs the existent XRD peak positions are displaced and broadened and the new XRD pattern appears in the neck region (curve 4, see arrows). Shifting of the diffraction lines (1 => 2 => 3) characterizes continuity of the stress-induced solid solution disintegration succeeded by phase transformation in critical point (4). This implies that the constant stress-induced creep at such a small isothermal strain (0.4% ε up to 200 h) is controlled by saturation of dislocation density because of the preferential contribution of lattice distortions (stored energy). Its critical value is a criterion of plastic instability at 0.5% ε. According to the findings and notions the widening of existent reflections testifies to dislocation density growth and stresses level increase while the displacement and appearance of new reflections testify to phase transformations [17, 18]. It is obvious that peak-broadening of all the X-ray lines and their shifts in XRD pattern (4) relative to ones (1–3) seems to interconnect not only with solid state phase transformation (essential change of phase composition), but also with increase of dislocation density during creep strain up to 0.5%. It can be seen that ever increasing amount of stored energy because of lattice distortion broadening is accumulated upon deformation while no essential change in crystalline size broadening appears to occur at such a small creep strain. Hence, peak broadening is entirely due to lattice distortions.

Development of creep strain at 423 K and 70 MPa is succeeded by saturation of critical lattice distortion (dislocation density) under tensile loading and, as consequence, dynamically unstable decomposition of α–Mg solid solution to initiate the tensile-stressed disperse phase transformations. Especially it is very clearly seen in the neck region that the plastic instability arises from creep strain of 0.5% (Fig. 5, curve 4). Thus, useful long-term strength is controlled by the critical time before building-up the neck under combined (three-axial) tension, which is responsible for starting of the accelerating stage of creep. In such a case the stable microstructure of the magnesium alloy based on Mg–Al–Ca–Y system is destroyed because of creep strain which is localized due to the necking in plastic instability condition. Reflections of unknown phase under 2θ–36°20(curves 1, 2, 3 Fig. 5) and 2θ–38°20(curve 4 Fig. 6) angles corresponding lattice spacings 0.247 and 0.237 nm, respectively, are observed. They fit neither α–Mg nor β–$Mg_{17}Al_{12}$ phase (Fig. 6).

The Mg–Al–Ca–Y and Mg–Al–Ca–Ti alloys exhibit significantly different behavior upon being creep strained. It is appropriate to compare the plot in Fig. 5 with ones shown in Figs. 6 and 7. XRD pattern of Mg–12.5Al–1.4Ca–0.28Mn–0.1% Ti in as-cast state demonstrates presence of many X-ray lines of small intensity, which may be connected with some insoluble quantities of second phase particles that are not observed after creep strain. It follows that the over-alloyable titanium atoms seem to be solved in α-Mg on the structural defects, namely dislocations, which could be chemically bounded with solute atmospheres by Cottrell hardening mechanism. In Fig. 6 XRD pattern shows additional X-ray lines (0002) and $\left(10\,\bar{1}\,1\right)$ near the reflection angles 2θ–38° and 40°, respectively. They are likely to be caused by presence of an additional phase as a result of over-alloying. It should be underlined that after strain the X-ray lines (0002) and $\left(10\,\bar{1}\,1\right)$ disappear by reason of the phase dissolution with increasing the strain-induced dislocation density. The results obtained are in a good agreement with the amplitude-dependent internal friction date (Fig. 3), which is in favor of pinning the dislocation structure with binding energy of about 0.3 eV (Table 3). Low dislocation mobility requires a higher driving stress for creep strain to occur without any phase transformations. Promising alloying elements such as titanium that possesses effective solubility on structural defects in α–Mg (Figs. 2 curve 6 and 3) are capable of binding moving dislocations and thereby to play the role of traps delaying the formation of critical dislocation density during creep deformation as much as 200 h. There is evidence that jerky flow (Fig. 8) and other yield point phenomena trigger activation of the rate-controlling mechanism [11, 34]. In the course of tensile tests, serrations typical of the Portevin—Le Chatelier effect are observed in magnesium alloys containing Ti, Sr, Gd additions at stress rate of about 10^{-3} s^{-1}. The a.e. of the phenomenon which controls the appearance of the serrations is comparable to vacancy migration energy (∼0.8 eV), while the energy governs its disappearance is similar to self-diffusion energy (∼1.35 eV).

It is noteworthy that jerky flow (the Portevin–Le Chatelier effect) occurs while introducing the AE such as Ti and et sec. with large positive heat (enthalpy) of mixing, ΔHm. For Mg–Ti system ΔHm makes up 16 kJ/mole [35]. The measurable effect of jerky flow is determined by the serrations on the smooth curve $\sigma - \varepsilon$ at $\dot{\varepsilon} = \text{const}$ (Fig. 8). This should be considered as indication of some limited dislocation activity due to pinning the dislocations by Cottrell mechanism with formation of dislocation atmospheres. Jerky flow in Ti-containing magnesium is observed during tensile tests. With this provision, regular serrations are certain to occur in the temperatures range of 403–523 K.

Power creep law relation and thermally activated behavior

As is well-known, temperature-dependent (Arrhenius behavior) and stress-dependent (power low) steady state creep rate, $\dot{\epsilon}_s$ are described by the following relationship:

$$\dot{\epsilon}_s = A\sigma^n \exp(-Q_c/RT) \quad (4)$$

where Q_c is the a.e. for creep; n is the stress exponent; A is a constant. The parameters, n and Q_c, are related to the dominant (rate-controlling) mechanism of creep deformation, which depends on applied stress and temperature. Therefore, abrupt changes in Q_c and n may be found when the dominant creep mechanism changes. The experimental results from tests at 423 K for all stresses (up to 90 MPa) show a reasonable fit to a straight line with different stress exponents in the appropriate stress ranges (Fig. 9). According to [36] n is equal to 1…2 if diffusion creep is rate-controlling mechanism, $n \sim 3$ for some solid solutions and $n \sim 4\ldots5$ for many other alloys and pure metals. Here it is thought that microdeformation mode below

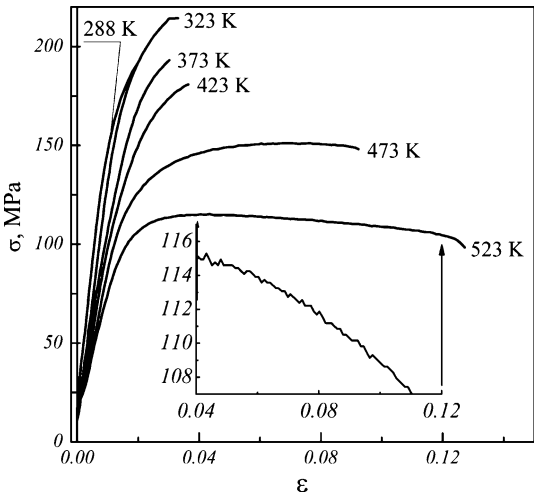

Fig. 8 Repeated (serrated) yielding in Mg–12,5Al–1.3Ca–0.4Mn–0.2Ti alloy during short-range tensile test

Table 3 Binding energy E_b as function of alloy composition

Alloy designation	Mg (99.96%)	Mg–12.5Al–1.2Ca	Mg–12.5Al–1.3Ca	Mg–12.5Al–1.4Ca–0.28Mn–0.1Ti	Mg–4.9Al–0.28Mn–1.8Sr
Eb, eV	0.21	0.32	0.50	0.27	0.21

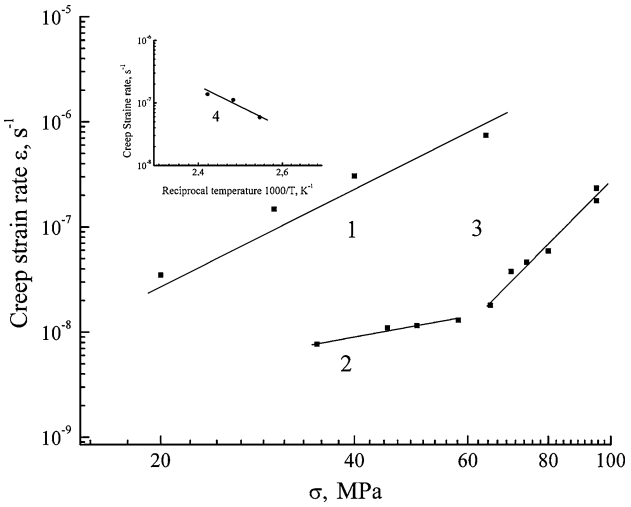

Fig. 9 Dependence of measured steady state creep strain rate on applied stresses at 423 K (power law) for different magnesium-base alloys: *1* AZ91D (Dow Chemical Corp., USA) ($n \sim 3$), *2* Mg–12.5Al–1.4Ca ($n \sim 2$), *3* Mg–12.5Al–1.4Ca–0.3Y ($n \sim 6$). *Inset* Arrhenius plots in the power low creep regime for Mg–12.5Al–1.4Ca alloy with a.e. of 0.8 eV

macroscopic yield is controlled by dislocation creep [37]. Alloys of Mg–Al–Zn, Mg–Al–Ca, and Mg–Al–Ca–Y exhibits a pronoun power law creep regime with no stress threshold to demonstrate solid solution strengthening for AZ91D ($\sigma \approx 20$–60 MPa) and Mg–12.5Al–1.4Ca alloy ($\sigma \approx 30$–60 MPa) (Fig. 9, curves 1 and 2). For Mg–12.5Al–1.5Ca–0.3Y alloy $\dot{\varepsilon}_{\text{п}}$ obeys a power low $\dot{\varepsilon}_{\text{п}} \infty \sigma^n$, where $n \approx 6$ (Fig. 9, curve 3). Such values of the stress exponent, n are typical for high temperature dislocation creep mechanism accommodated most likely by solute diffusion of the Y to the dislocations. Indeed, dislocations initiated at the interface (Fig. 1b) control creep resistance followed by power law at higher temperatures [36].

Temperature dependence of the creep rate $\dot{\varepsilon}$ is shown in the Arrhenius plots of Fig. 9, curve 4. The slope of the straight line relationship multiplied by K (gas constant) gives the apparent activation energy for creep, a.e. Q_c to be equal of about 0.8 eV for the magnesium-base alloy of Mg–Al–Ca system at 64 MPa. Unlike Al, Mn, and Zn the alloying by Ca as slower-diffusing substitution element enhances contribution of the accommodated mechanism of GB-diffusion in segregated alloy (Fig. 2, curve 2), thus increasing a.e. of diffusion from 0.3 to 0.4 eV (GB-self diffusion in HCP Mg) to 0.7–0.9 eV upon additional alloying by Ca. It is important that the value coincides with a.e. required for migration of vacancies. At larger stresses (60–90 MPa) (Fig. 9, curve 3) creep strain rate for magnesium alloy of Mg–Al–Ca–Y system is the most likely to be controlled by bulk (lattice) dislocation climb ($n = 3$–6). For reasons given, corrections to the chemical composition in Mg–Al–Ca system was carried out to improve the solid solution strengthening and creep resistance of the magnesium alloys in terms of new ratio of Al to Ca [38, 39] and additional alloying with promising elements such as Ti, Sr, and Gd.

Creep resistance and long-term strength

The greatest advantages of new experimental alloys were revealed during creep tests. As can be seen from Table 4 and Fig. 10, at 423 K under stress of 70 MPa they exhibit creep strain which grows significantly less than that of AZ91D and AE 42 magnesium alloys. Furthermore, their creep rate ($\dot{\varepsilon} \sim 10^{-9}$ s^{-1}) makes up value which is on two order of magnitude less than that of AZ91D alloy ($\dot{\varepsilon} \sim 10^{-7}$ s^{-1}) at a much less value of creep stress, 35 MPa. It is considered that in order to design for good creep resistance the recovery and softening effects should be minimized [40]. Shape of curves after tensile tests at r.t. and 423 K is found to be comparable with shape of creep curve at 423 K (Fig. 10). This implies indicates that creep strain in the newly developed magnesium alloys based on the ternary Mg–Al–Ca system is accumulated exhibiting deformation strengthening without recovery.

The significantly higher creep properties of magnesium alloy containing inexpensive addition of Sr (1.8%), Gd (0.2%) and very small addition of Ti (0.1–0.2%) (Fig. 11; Tables 4 and 5) differ favourably from AE42 alloy containing expensive additions of 2–3% RE that provides $\varepsilon_{\Sigma} \sim 0.84\%$ for 200 h at 423 K/70 MPa. Stress-induced effective solubility of α–Ti atoms on dislocations causes effect of self-strengthening for the inexpensive Mg–12.5Al–1.4Ca–0.3Mn–0.1Ti alloy thereby improving its useful long-term strength during creep strain at 423 K. Under such conditions creep limit amounts to 70 MPa at creep strain $\varepsilon_{\text{п}}$ no more than 0.5% and $\dot{\varepsilon}_{\text{п}}$ of about 10^{-9} s^{-1} during up to 200 h.

It is important to emphasize that long-term features exhibit some correlation between creep strain rate $\dot{\varepsilon}_c$ and time to a given creep strain (Table 4, Figs. 9 and 10) for all alloys under investigation. Somehow or other $\dot{\varepsilon}_c$ level indicates their survival probability. The authors abandon themselves to the idea that one should not carry out all the cycle of creep testing (up to 200 h) to save time and resources provided single rate-controlling mechanism will be operate. The proximate analysis unambiguously displays source data as creep strain rate rather that time interval. It might therefore be expected that solute-induced dragging is the most probable rate-controlling mechanism responsible for delaying the dislocation activity on the 10^{-9} s^{-1} level. This assumption is supported by appearance of regular serrations on the smooth curve during tensile test of magnesium alloy containing T_i addition

Table 4 Creep strain rate $\dot{\varepsilon}_s$ at 423 K as function of chemical composition

Alloy composition (destination)	Creep strain rate $\dot{\varepsilon}_s$, s^{-1}	Creep strength, MPa	t, h	Creep strain, ε, %
AZ91D (Dow Chemical Corp., USA)	10^{-7}	35	200	2.50
		64	100*	
Mg–12.5Al–1.3Ca	10^{-8}	64	200	0.35
Mg–12.5Al–1.3Ca–0.3Y	10^{-8}	70	48	0.40
Mg–12.5Al–1.3Ca–0.3Y–0.2Gd	1×10^{-9}	70	200	0.40
Mg–12.5Al–1.3Ca–0.3Mn–0.1Ti	1×10^{-9}	70	200	0.55
Mg–12.5Al–1.3Ca–0.3Mn–0.2Ti	1×10^{-9}	70	200	0.28

* Fracture

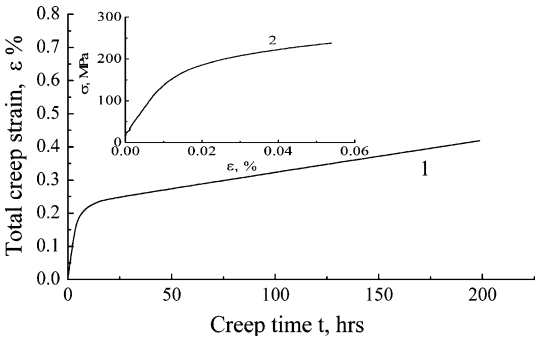

Fig. 10 Short-range and long-term properties of the newly developed magnesium-base alloy Mg–12.5Al–1.4Ca–0.3Y–0.2Gd: *1* creep curve at 423 K/70 MPa for 200 h, *2* typical tensile strain–stress curve at 203 K

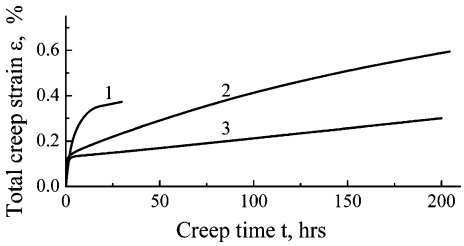

Fig. 11 Creep curves for magnesium alloys containing titanium (in %): Mg–12.5Al–1.4Ca–0.3Y–0.07Ti (*1*), Mg–12.5Al–1.4Ca–0.28Mn–0.1Ti (*2*), and Mg–12.5Al–1.3Ca–0.4Mn–0.2Ti (*3*)

Table 5 EDXS analysis of elementary composition of the fracture surface at 293 K for the tensile stressed Mg–12.5Al–1.3Ca–0.3Mn–0.1Ti alloy

Element	wt, %	at, %
Mg	18.68	25.69
Al	39.36	48.76
Ti	0.28	0.19
Cr	0.36	0.23
Mn	40.02	24.35
Fe	1.30	0.80
Total	100.00	100.00

(Fig. 8 and Table 5) as well as by dislocation damping investigations (Figs. 3 and 4).

Discussion

Analysis of ongoing magnesium alloy development activities throughout the world indicates current efforts in the development of die, Ca-containing and modified casting alloys with improved elevated-temperature properties and with acceptable cost to the automobile industry [41–45]. The main reason of slow inculcation of magnesium alloys on the automobile market is insufficient castability, high cost and insufficient reproducibility of their properties. From the point of view of the Dead See Magnesium Ltd; and Volkswagen A.G. joint research group, requirement of low cost along with castability problems reduces possible options to alloy systems containing Al or Zn as principal alloying elements, with using Mn, Si, Ca, and Sr as relatively small additions as well as Ce or La-based mish-metal [1, 2].

Mg–Al–Ca system: general characterization

A sufficient amount of Al in the magnesium alloy melt is considered to provide its good die-castability properties. At the same time formation of eutectic corrosion-resistant $Mg_{17}Al_{12}$ intermetallic results in decreasing the creep resistance. As is well-known, replacing RE with Ca for magnesium alloys in Mg–Al system could lower their cost without impairing the mechanical properties. The same level of creep resistance for AX 51 alloy in Mg–Al–Ca system containing the strengthening phase Al_2Ca is produced at much lower cost than for AE 42 alloy containing RE element (Ce) [3]. Nevertheless, the current commercial magnesium alloys of the Mg–Al and Mg–Al–Zn systems making up the bulk of those used in automotive industry do not exhibit creep resistance while maintaining die castability and room temperature strength. The second group of these alloys in Mg–Al–RE and Mg–Al–Si systems offers

borderline improvement in creep resistance but cost and poor die castability are their main disadvantages. Except for the Mg–Al–Ca and Mg–Zn–Al–Ca systems other patent experimental alloys also contain the expensive rare earth additions [46, 47]. The less expensive Mg–2…6%Al–0.25…5.5%Ca with composition to give Al_2Ca precipitation [46] has had die castability problems including hot tearing when prototyping an automatic transmission case. A subsequent version of the alloy, Mg–Zn–Al–Ca has had promise in eliminating die cast problems but the alloy seems to work only in an extremely narrow composition range and also to exhibit variation in properties. Thus, more data have to be generated on present and newly developed types of alloys to confirm that magnesium product is a serious candidate for the desired applications (running gear, engine blocks, etc.).

Comparable data analysis

Before proceeding to a presentation of the approach it should be pointed out that X-ray data considered here are limited to the analytic potentiality of the X-ray diffraction method, as is clearly shown in Figs. 5, 6, 7. In particular, some X-ray lines (for example, line of Ti at 38°, etc.) on the XRD patterns have disappeared (Figs. 6 and 7). In addition to this, the traces of other phase are observed as four lines with reflecting angles 30.6°; 34.8°; 37.7°; 38.3°. In some samples the 34.8°—peak is imposed on the (002) peak of HCP Mg lattice. These additional lines may be identified within the framework of hexagonal cell with $a = 0.2770$ nm and $c = 1.6454$ nm or of ortorombic cell with $a = 0.2770$ nm; $b = 0.2921$ nm; $c = 1.4100$ nm. Such being the case it is very difficult to carry out the thorough X-ray diffraction analysis and to obtain exact structural determinations regarding the behavior of almost insoluble T_i in HCP Mg by analyzing X-ray evidence only. In a word, the authors are not able to defect decomposition of α–Mg solid solution in its early stages and to analyse behavior of small additions by reason of limiting accuracy of X-ray diffraction analysis. At the same time Q^{-1} experimental technique is capable of improvement in accuracy. In fact the damping measurement (Figs. 2, 3 and 4; Tables 2 and 3) is a true reflection of the observed behavior of magnesium alloys in Mg–Al–Ca system containing small additions of Ti and Sr.

The principal part of the discussion is therefore concerned with the $Q^{-1}(T)$ changes which occur during successive alloying with the additions under investigation. Detailed structure consisting of GB dislocations is vitally important in understanding GB sliding and creep properties of the magnesium alloys studied. Some localized strain is apparent at the interface (Fig. 1b). The evidence for GB sliding derives principally from damping measurements (Fig. 2). The experimental profile and experimental points (around 458 K) of the maximum in HCP Mg (Fig. 2, curve 1) seem to follow GB inelastic relaxation, which is very similar to that already found for the GB peak in doubly sublimated HCP Mg of high purity at 1 Hz [27]. The height of the GB Q^{-1} maximum is approximately proportional to the GB dislocation density. This maximum is thermally activated and characterized by a.e. of 1.3 eV. GB contribution of the dislocations to GB sliding has totally suppressed in Mg–Ca alloy.

In the periodic literature [27, 28, 48–51] discussion is essentially based on correlation between the GB relaxation and the intrinsic GB sliding. It has been previously shown [49] that GB internal friction in HCP Zn to be resolved in two components is associated with diffusive motion of GB dislocations. A similar interpretation was used to explain the features of GB dislocation-induced relaxation and GB solute segregation-induced relaxation in HCP Mg (Fig. 2). Detailed considerations of the two mechanism of damping are discussed in another paper [48, 50, 51]. The mechanism of extrinsic GB sliding discussed so far is consistent with an analysis of the GB relaxation phenomenon occurring along GBs and with a real origin of the new kind of GB relaxation observed (Fig. 2). It should be pointed out that the first broad $Q^{-1}(T)$ maximum is overlapped by some small peaks of the dislocation origin, answering the description of Fig. 2 (curve 1) in Internal friction measurements.

Following the data of mechanical spectroscopy [48] two GB peaks are found to be present in the temperature-dependent damping spectrum of the Mg–3%Ni alloy. First of them is ascribed to thermally activated dislocation relaxation, while second $Q^{-1}(T)$ peak seems to be attributed to the GB solute relaxation.

Softening effect of grain boundary sliding in HCP Mg polycrystals arises in the stress-temperature ranges of interest for automotive applications. Furthermore, precipitation from the saturated α–Mg solid solution is succeeded by deterioration of their properties during creep. These two main effects are the most likely to decrease creep resistance and long-term strength of magnesium alloys in Mg–Al–Mn and Mg–Al–Zn systems. It is considered that in order to design for good creep resistance the recovery and softening effects should be minimized. Poor creep resistance of HCP Mg is enhanced by increase in macroscopic sliding due to existence of the relaxing GB dislocations in its polycrystal. The apparent complexity of the grain boundary internal frictional maximum for HCP Mg (Fig. 2) seems to preclude a detailed description of the dissipation mechanism.

Nonequilibrium grain boundaries provide a large number of excess dislocations for slip [52, 53]. GB dislocations and back stress were used to account for large

stress-exponent $n \approx 2\ldots5$ [54]. Following the calculated data the solutes in the GBs effectively retard the GB dislocation-induced relaxation (Fig. 2) thus significantly decreasing both the minimum creep rate and creep strain, as one should be expected.

According to [55, 56] Ti possesses the largest positive enthalpy of mixing (making up 16….30 kJ/mole for bimetallic system Mg–Ti) and therefore is considered as insoluble alloying element relative to HCP Mg. Nevertheless, the authors have revealed 0.28 wt, % (0.19 at, %) Ti in magnesium alloy using rapid solidification method (Table 5).

One of the reason for structure instability in the course of dynamic strain ageing (DSA) is the stress-induced and structure-sensitive interaction between mobile dislocations and diffusants (solute atoms). Under these conditions the corresponding Portevin–Le Chatelier effect is succeeded by the sharp decrease in the creep strain, with negative strain rate and positive temperature dependence of the flow stress [57]. Observed post relaxation effect because of DSA is caused by the change in the concentration of solute atoms on dislocations with the temperature and strain rate. Unlike slow kinetics of solid solution disintegration kinetics of segregation of solute elements or their desegregation are extremely rapid, suggesting short-range diffusion of segregant [58]. Thus, the only causes for the huge decrease in creep rate could be: (a) a decrease in the bulk (lattice) diffusion coefficient due to introducing more refractory additions, and/or (b) a slowdown in dislocation activity due to solute-induced dragging.

It is reasonable to expect that the excellent increase in creep resistance and long-term strength should be attributed to dynamic (stress-induced) dragging the dislocations by non-equilibrium Cottrell's dislocation atmospheres in full-accordance with physico-chemical Le Chatelier-Broun principle of mobile equilibrium [59].

There is an evidence that jerky flow (effect of the Portevin–Le Chatelier) is occur while introducing the alloying elements with large positive heat (enthalpy) of mixing. The measurable effect of jerky flow is determined by the serrations on the smooth curve $\sigma - \varepsilon$ at stress rate $\dot{\varepsilon} = \text{const}$ (Fig. 8). This should be considered as indication of some limited dislocation activity due to pinning the dislocations by Cottrell mechanism with formation of dislocation atmospheres. Jerky flow in Ti-containing magnesium is observed during tensile tests ($\dot{\varepsilon} = 10^{-3}$ s^{-1}). With this provision, regular serrations are certain to occur in the temperatures range of 403–523 K.

The activation energy (a.e.) of the phenomenon which controls the appearance of the serrations is comparable to vacancy migration energy ($\sim$0.8 eV), while the energy governs its disappearance is similar to self-diffusion energy ($\sim$1.35 eV) [60]. The point defects are generated during straining by the non-conservative motion of jogs on mobile dislocations. Following the modified versions of Cottrell model for the Portevin–Le Chatelier effect [61] it is deduced that repeated (serrated) yielding is caused by short-range diffusion of clusters "excess vacancy-solute" which insure the dislocation locking with the participation of the strained-produced vacancies. Annealing of the excess vacancies at appropriate sinks or their annihilation give rise to deviations of experimental data from Cottrell model by primary cluster-induced mechanism [29].

It is important to emphasize that long-term features exhibit some correlation between creep strain rate $\dot{\varepsilon}_c$ and time to a given creep strain (Table 4, Figs. 9, 11) for all alloys under investigation. Somehow or other $\dot{\varepsilon}_c$ level indicates their survival probability. The authors abandon themselves to the idea that one should not carry out all the cycle of creep testing (up to 200 h) to save time and resources provided single rate-controlling mechanism could be operate. The proximate analysis unambiguously displays source data as creep strain rate rather than time interval. It might therefore be expected that solute-induced dragging is the most probable rate-controlling mechanism responsible for delaying the dislocation activity on the 10^{-9} s^{-1} level. This assumption is supported by appearance of regular serrations on the smooth curve during tensile test of magnesium alloy containing Ti addition (Fig. 8) as well as by dislocation damping investigations (Figs. 3 and 4).

New outlook for magnesium alloy development

Thermal analysis indicates that temperatures of phase transformations depend on the chemical composition of new experimental magnesium alloys consisting of low-cost AE. Kinetics of their decomposition and bulk cooling rate under their solidification by crystallization is accessed through 333 K/s [26, 34, 39, 47]. By reason of the rapid solidification rates experienced during pressure die casting the magnesium alloys of Mg–Al system such AM50, AM60 as well as AZ91D are affected by supersaturation of α–Mg solid solution in as-cast condition. Moreover, due to the divorced nature of their eutectic they are laminated to form regions of highly supersaturated α-Mg adjacent to the GBs. This leads to an unstable microstructure and extensive precipitation that continues for many hundreds of hours.

The slow kinetics of the thermal decomposition gives rise to keeping metastable α–Mg matrix solid solution and to decreasing creep resistance of commercially available alloys based on the Mg–Al system [62]. Addition of Ca under know-how ratio of Al to Ca [39] results in stabilization of α–Mg solid solution in the Mg–Al–Ca alloy system. At the same time, fast kinetics of segregation/desegregation restricts long-term strength at 423 K for

200 h to the creep strength of 64 MPa (Table 4). Nevertheless, alloying of magnesium with the greater quantity of aluminum (up to 12.5 wt%) leads to an increase in its castability (up to 30%). This allows to use the family of magnesium alloys for manufacturing the parts which are very difficult to cast. Besides, increasing the Al content (nearer to eutectic point) leads to a doubling in the volume fraction of dispersed eutectic structural component β–$Mg_{17}Al_{12}$ to be strengthened by solute third AE (Tables 1 and 4).

There are two bimetallic magnesium-base systems of different kind with negative and positive enthalpy of mixing. The vast majority of them are formed in the systems with negative heat and enthalpy of mixing (e.g., Mg–Zn, −4 kJ/mole; Mg–Si, −26 kJ/mole; etc.) due to the reduction of Gibbs free energy upon intermixing to form solid solution or intermetallic compound [55]. A large negative heat of mixing in the liquid characterizes a high glass-forming ability for metallic alloys. At the same time Mg–Ti system relates to positive heat-of-mixing metallic systems which have not a thermodynamic driving force [56] and is characterized by a large positive heat of mixing (16 kJ/mole) in both the liquid and solid states according the Miedema model [63].

As is known, systems with a positive heat of formation (enthalpy of transformations to standard elements) tend to favour "de-mixing" [64] as well as to local ordering. For reasons given their formation requires very high cooling rates: local structure evolves rapidly requiring mostly short-range diffusion and arrangements. However, rapid kinetics of Ti (Gd, Sr) microsegregation under a high-speed treatment is at variance with the slow kinetics of the thermal and stress-induced decomposition. By doing so the mobile fluctuations of chemical composition promote to the dislocation pinning. Unfortunately, in the study of the systems to date, convincing evidence is generally lacking in establishing the exact extent of alloying of the atomic-level homogeneity [65, 66]. Multi-component additions may have changed the magnitude or even sign of the heat of mixing so that their incorporation should be carried out on segregation-level scale due to the rapid solidification-induced dislocation structure. In order to alloy a pair of constituent ("immiscible") elements revealing little or no mutual solubility even in liquid state up to very high temperatures it is necessary to employ highly non-equilibrium processing that overcomes a solubility barrier, for example, through the rapid quenching route. In order to solve the problem in the multicomponent Mg–12.5Al–1.3Ca containing 0.1–0.2 wt% Ti the authors have used for the first time a processing technique of rapid quench from solid phase rather than mechanical alloying [67] that is unsuitable for die-casting technology. Rapid solidification rate in the experiments closely resembles that to be expected from die-casting procedure (up to 373 K/s). Moreover, the approach provides the extent of atomic-level alloying with Ti, Sr, Gd, etc., due to as-cast dislocation structure having binder and accommodation capacity on the atomic segregation-level.

The Mg–X systems (where X–Gd, Sr) should be likened to those bimetallic systems with particular thermodynamic properties seeing that the same causes produce the same effects. As one should expect, this approach is in agreement with the well-known Le Chatelier-Broun principle of mobile equilibrium which is useful in the linear thermodynamics of non-equilibrium processes [68].

Principles of alloying of the newly developed magnesium alloys

A physically based constitutive model of dislocation creep retardation is suggested, based on the structural-energy efficiency concept of useful long-term strength valid for metal alloy systems. It takes account of physical defect kinetics, i.e., speed change and dislocation dragging by Cottrell solute atmospheres consisting of slower diffusing refractory AE with special thermo-dynamic properties. Upon small-scale alloying they exhibit large positive values of enthalpy of mixing (16….30 kJ/mole for Mg–Ti system [55, 56]), a tendency to clustering a structure of α–Mg solid solution and effective solubility on dislocations in the non-equilibrium conditions crystallization thereby overcoming a barrier of their solubility. The approach gives rise to elucidate the physical nature of titanium beneficial effect, which is attributed to an occurrence of limited-mobility dislocations in the high-stress regime. These notions are supported by experimental observations including the ADIF measurements (Figs. 3 and 4), discrete temperature spectra change (Fig. 2), X-ray diffraction analysis (Figs. 5, 6, 7) and repeated (serrated) yielding (Fig. 8).

Novelty of the approach consists in development of physical principles of precision (on atomic-energy level) alloying of Mg–Al–Ca matrix with promising additions having a large positive enthalpy of mixing using processing technique of rapid solidification. They are based on high sensitivity of the selected alloying elements such as Ti, Gd and Sr to the solidification/cooling rates. This makes it possible to overcome a potential barrier of solubility in the non-equilibrium conditions and facilitates introducing in a melt of the additions insoluble in equilibrium conditions.

Any die-casting process is succeeded by rapid solidification of a magnesium melt the rate of which hesitates within the limit of 313…333…373 K per second. The relevant dislocation structure to be formed in as-cast condition can be expected to interact only with the fast-acting

alloying elements which are able to trap the dislocations in the non-equilibrium conditions of crystallization. Original idea is to select those of them which will be able to inhibit the initiation of critical dislocation density responsible for deterioration of creep properties at higher temperatures and thereby to enhance contribution of the refractory metal diffusion responsible for increase in heat resistance. It is these alloying elements such as Ti, Gd, and Sr that can do it having negligible or low lattice solubility in HCP magnesium (α–Mg) at elevated temperatures. Being that the AE exhibit high sensitivity to the high-speed treatment they can be expected to increase effective solubility (on structural defects) thereby extending limit of their solubility. This effect is succeeded by essential pinning of moving dislocations with solute atmospheres by Cottrell hardening mechanism [11]. Its activation in the stress field should minimize solute effects to increase creep resistance and long-term strength up to 70 MPa at 423 K for 200 h with slow creep rate at 10^{-9} s^{-1}.

It is considered [39, 40] that magnesium alloys of Mg–Al–Ca system suffer from creep caused by both dissolution-diffusion change and thermal decomposition. However, new information provided for multicomponent (quaternary) Mg–Al–Ca–Ti and Mg–Al–Ca–Sr systems forms a strong basis for magnesium alloy design concept based on preferential contribution of stress-induced decomposition and stress-induced diffusion-controlled reactions to occur during long-term creep testing (Figs. 2, 5, 6, 7, 10, 11). In this case dissolution of the AE occurs on the structural defects such as dislocations. As such, solute atmosphere dragging becomes rate-controlling mechanism responsible for improvement of creep properties and heat resistance (Figs. 2, 9, 10, 11) based on Cottrell hardening (Figs. 3, 4, and 8). The idea of self-strengthening is supported by XRD analysis of the microstructure after creep strain at 423 K/70 MPa (Figs. 5, 6, 7).

To summarize in a few words, the main advantages of the newly developed experimental magnesium alloys are reduced to the following:

1. *castability* is considered to be the main critical property of any die-casting alloy. Higher castability (up to 30%) and good melt handling of the newly developed Al-rich magnesium alloys compared to the commercial alloys AZ91D, AE42, and AS21 is insured by new ratio of Al/Ca which has been patented. Due to Al-rich compositions the magnesium alloys under investigation are intended to parts which are very difficult to cast;
2. *higher creep resistance and long-term strength* the newly developed magnesium alloys of Mg –Al–Ca–Ti and Mg–Al–Sr–Ca–Ti and Mg–Al–Ca–Y–Gd systems are found to have the best combination of room and creep temperature properties revealed by successful short-range and long-term range tensile testing at 64…..70 MPa and 423–448 K. Their appropriate compositions covered by patent pending due to basic matrix Mg–Al–Ca patented in Ukraine. Their creep properties at 403–423 K under stress of 50–70 MPa are significantly better than that of the commercial alloys AZ91D, AE42, and AS21. Unlike a AZ series of magnesium alloys with divorced cutectics (AZ91D, etc.) the new experimental magnesium-base alloys containing cheaper additions compare favourably with higher creep and heat resistance as well as long-term strength compared to magnesium alloys AS21 (Mg–2%Al–1.5%Si), and AE42 (Mg–4%Al–2.5%RE) containing expensive additions, in the temperature and stress ranges of interest for automobile applications.
3. *longer life* creep strength of Mg–12.5Al–1.3Ca basic matrix is found to be 64 MPa. The creep strength is increased up to 70 MPa upon its alloying with small additions of Ti and etc. A new family of creep-resistant and long-term strength presents a cost-efficient system capable to operate at 70 MPa/423 K for 150–200 h with allowance of total creep strain 0.2….0.4….0.6%.

Conclusions

The basic conclusions to be drawn from the results obtained may be stated as follows:

- following the data of internal friction measurements the introduction of Ca is found to suppress grain boundary relaxation to promote the grain boundary strengthening of magnesium alloys in the ternary Mg–Al–Ca system. Increasing the Al content to 12.5% wt% and to fractional increase of Ca content leads to a doubling in the volume fraction of the second eutectic component β–$Mg_{17}Al_{12}$ to be strengthened. Lattice distortions in the both α–Mg solid solution and β–$Mg_{17}Al_{12}$ are compositional-dependent. Such a structure enhances contribution of natural eutectic strengthening;
- X-ray studies reveal the structural and phase transformations that arise during long-term creep testing in the neck of a specimen; the critical residual stored microstrain is found to be responsible for the localized necking which should be regarded as physical limitation of useful long-term strength of magnesium alloys in system Mg–Al–Ca–Y;
- introduction of small additions of Ti (about 0.1–0.2%) and large amount of Sr (up to 1.8%) within the basic melt causes significant solid solution strengthening due to pinning of slowly moving dislocations by the Cottrell atmosphere mechanism with binding energy of about

0.2–0.3 eV. Titanium having a large positive enthalpy of mixing is introduced in matrix for the first time using processing technique of rapid quench (up to 373 K/s) from high-temperature solid phase;

- following the internal friction measurements the alloying of the Mg–Al–Ca basic matrix with more refractory additions such as Ti and Sr extends the temperature range of their interaction with pre-existing dislocations increasing high-temperature strength of the Mg–12.5Al–1.3Ca–0.3Mn–0.1Ti and Mg–4.9Al–0.3Mn–1.8Sr alloys by 393–533 K due to the formation of phase and thermally stable structure;
- it is deduced that resulting dynamic structure to be formed during creep straining appears to be responsible for improvement of the observed creep resistance and long-term strength due to thermally activated dislocation relaxation accommodated by diffusion of alloying elements (Al, Ca, Ti, Gd, Sr in their best combination);
- an excellent increase in creep resistance and long-term strength at higher temperatures and larger stresses (70 MPa at 423 K) is provided by solute-induced dynamic dragging (retardation) of dislocations moving at $\dot{\varepsilon}_c \sim 10^{-9}\ s^{-1}$. The finding is in agreement with the Le Chatelier-Broun principle of mobile equilibrium;
- the physico-chemical principles of precision (on segregation-energy level) alloying are suggested for so-called immiscible systems with a large positive heat of mixing and high sensitivity of the selected refractory alloying elements (Ti, Gd, Sr) to high-speed treatment to get their effective solubility on structural defects such as dislocations. From this point of view, three of the most promising alloys designated as UKOR–C1 (Mg–12.5Al–1.3Ca–0.3Mn–0.1Ti), UKOR–C2 (Mg–12.5Al–1.7Sr–0.3Mn–0.1Ti) and Mg–12.5Al–1.4Ca–0.3Y–0.2Gd (UKOR-C3) having excellent short-range mechanical properties (157-174 TYS, MPa; 239-268 UTS, MPa at r.t. and 153-206 MPa at 423 K; true fracture stress 240-265…292 MPa at r.t. and 229 at 423 K; 4.8 Elong., % and 6.7 Red.A. at F., %) can be selected for upscale production and further investigation to subject them to detail examination as to the die-castability, fluidity (die filling), sticking in die, susceptibility to hot cracking and porosity formation. Titanium as know-how alloying element is competitively able to strontium and attracts desirable properties changing solid-solution effects at ambient temperatures and increasing heat resistance.

Acknowledgements The authors would like to thank Prof. Britun V.F. for his continued interest to the problem, Dr. Malka A.N., Dr. Friesel V.V. and Dr. Chriplivy A.A. of the Institute for Problems of Materials Science, Ntl Acad. Sci., Ukraine for useful discussion and for supplying the necessary materials. The financial support have received from the Korea Government Foundation is gratefully acknowledged.

References

1. Aghion E, Bronfin B (2000) Mat Sci Forum 350–351:19
2. Bronfin B, Aghion E et al (2003) In: Kainer KU (ed) Proceedings of 6th international conference on magnesium alloys and their applications. Wiley, New York
3. Pekguleryuz MO, Renaud J (2000) In: Kaplan HI, Hryn JN, Clow BB (eds) Magnesium technology. TMS, Warrendale
4. Schmid-Fetzer R, Grobner J (2002) In: Proceedings of 6th international conference on magnesium alloy and their applications. Wiley, New York
5. Pekguleryuz M et al (2003) J Adv Mater 35:32
6. Luo A, Shinoda T (1999) US Patent US 5855997
7. Tkachenko VG et al (2003) Powder Metall Met Ceram 42:268
8. Breiman EM et al (1972) Met Trans 3:211
9. King JF (1998) In: Mordike BL, Kainer KU (eds) Proceedings of international conference on magnesium alloys and their applications. Werkstoff Informationsgesellschaft, Frankfurt
10. Hirsch PB, Howie A et al (1965) Electron microscopy of thin crystals. Butterworth's, London
11. Yoshinaga H, Morozumi S (1971) Phil Mag 23:1351
12. Smola B, Stulicova I et al. (2003) In: Kainer KU (ed) Proceedings of 6th international conference on magnesium alloys and their applications. Wiley, New York
13. Su CM, Ke TS (1986) Phys Stat Sol A94:191
14. Schoeck G, Bisogni E (1964) J Shyne Acta Metall 12:1466
15. Read TA (1940) Phys Rev 58:371
16. Th H, de Keiser JI, Landford EJ, Mittemeijer ABP, Vogels (1982) J Appl Cryst 15:308
17. Taylor A (1961) X-ray metallography. John Wiley and Sons Inc., New York
18. Krivoglaz MA (1996) X-ray and neutron diffraction in nonideal crystals. Springer Verlag, Berlin
19. Lund RW, Nix WD (1976) Acta Metall 24(5):469
20. Massalski TB (1965) Physical Metallurgy, RW Cahn, Charter III. North-Holland, Amsterdam
21. Rossouw CJ, Venkatesan (2001) J Electron Microscop 50(5):391
22. Michael M (ed) (1999) ASM Specialty handbook. Avedeslan and Hude Beker, ASM Int., Materials Park, p 8
23. Murray JL (1982) Bull Alloy Phase Diagrams 3:335
24. Ryum N (1968) Acta Metall 16:327
25. Tkachenko VG, Strongin BG et al (1996) Int J Hydrogen Energy 21:1091
26. Tkachenko VG (2009) Prog Phys Metal 10:103 (in Rus)
27. Delaplace J, Nicoud JC, Trabut L (1970) J Nuclear Mater 35(2):167
28. Buzzichelli G (1969) Solid State Commun 7:1347
29. Tkachenko VG, Shuljak II, Strutinsky AM et al (2002) In: Veziroglu N et al (eds) Huddrogen materials science and chemistry of metal hydrides. Kluwer Academy, Netherlands, p 77
30. Tkachenko VG, Tatarenko VA, Shuljak II et al (2001) Metall Noveishie Teknol 23(3):367
31. Ke Trans TS (1986) Jpn Inst Met 27(Suppl):679
32. Pettersen K, Siedersleben J (1996) In: Proceedings of 15th International Pressure Die Casting Conference, Montreux
33. Uchida H, Shinya T (1995) J Jpn Inst Light Metals 45:572
34. Tkachenko VG (2002) Strength physics of less-common metals and their alloys, 2nd (ed) Cambridge Sci. London, Nauk D Kiev (1996, in Rus)
35. Inoue A, Takeuchi A, Zhang T (1998) Mater Trems A29:1779

36. Nabarro FRN, Devilliers HL (1995) The physics of creep. Taylor and Francis, London
37. Evans RW, Wilshire B (1985) Creep of metals and alloys. Institute of Metals, London
38. Tkachenko VG, Maksimchuk IN, Volosevich PYu et al (2006) High Temp Mater Process 25:97
39. Tkachenko VG, Malka AN, Maksimchuk IN et al (2007) Ukraine Patent 79413
40. Poirier J-P (1987) Creep of crystals. University Press, Cambridge
41. Park J, Kim M, Yoon U et al (2009) J Mater Sci 44(1):47. doi:10.1007/s10853-008-3130-z
42. Hakamada M, Shimizu K, Yamashita T et al (2010) J Mater Sci 45(3):719. doi:10.1007/s10853-009-3990-x
43. Shepelev D, Bamberger M, Katsman A (2009) J Mater Sci 44(20):5627. doi:10.1007/s10853-009-3793-0
44. Yang MB, Cheng L, Pan FS (2009) J Mater Sci 44(17):4577. doi:10.1007/s10853-009-3696-0
45. Wu RZ, Deng YS, Zhang ML (2009) J Mater Sci 44(15):4132. doi:10.1007/s10853-009-3605-6
46. Pekguleryuz MO, Luo A (1996) Patent application WO 96/25529
47. Luo S, Sinoda T (1997) US Patent 5855697
48. Diqing Wan, Yajuan Liu (2011) Adv Mater Res 146–147:1761
49. Bonetti E, Cavallini A, Evangelista E, Gondi P (1983) J de Physique 44:759
50. Woirgard J, de Fouquet J (1974) Scripta Met 8:253
51. Woirgard J (1976) Phil Mag 33:623
52. Hanaoui A, Van Suygenhoven H, Derlet PM (2002) Acta Mater 50:3927
53. Valiev RZ, Alexsandrov IV, Lowe TC (2002) J Mater Res 17:5
54. Yin WM, Whang SH, Mirshams RA (2005) Acta Mater 53:383
55. Inoue A, Takeuchi A, Zhang T (1998) Mater Trans A29:1779
56. Ma E (2005) Prog Mater Sci 50:413
57. Trojanova Z, Lukac P, Cizek L (2003) In: Kainer KV (ed) Proceedings of 6th international conference on magnesium alloys and their applications. WILEY-VCH, DGM, Wolfsburg, p 495
58. Westbrook JH, Wood DL (1961) Nature 192:78
59. Kheilova M, Strunc M (1995) J Non-Equilib Thermodyn 20:19
60. Dinhut JF, Banou T, Moire P (1976) Acta Metall 24(5):441
61. Murty K, Mohamed FA, Dorn IE (1971) Scr Metall 5:1087
62. Celotto S, Bastow TJ, Humble P et al. (1997) In: Proceedings of 3rd International Magnesium Conference. Institute of Metals, London
63. Boer FR, Boom R, Mattens WCh, Miedema AR, Niessen AK (1988) Cohesion in metals. Amsterdam, North-Holland
64. Crespo-Sosa A (2003) Mater Sci Eng B 100:297
65. Krack BD, Ozolins V, Asta M, Daruka I (2002) Phys Rev Lett 81:186101
66. Enrique R, Nordlund K, Averback RS, Bellon P (2003) J Appl Phys 93:2917
67. Liang G, Schultz R (2003) J Mater Sci 38:1179. doi:10.1023/A:1022889100360
68. Petrucci RH (1972) General chemistry: principles and modern applications, 1st edn. Macmillan, NY, p 275